Interplanetary Magnetic Holes: Theory

L. F. Burlaga

Laboratory for Extraterrestrial Physics, NASA/Goddard Space Flight Center, Greenbelt, Maryland 20771

J. F. Lemaire

Institut d'Aeronomie Spatiale de Belgique, B-1180 Brussels, Belgium

Magnetic holes in the interplanetary medium are explained as stationary nonpropagating equilibrium structures in which there are field-aligned enhancements of the plasma density and/or temperature. Magnetic antiholes are considered to be associated with depressions in the plasma pressure. In this model the observed changes in the magnetic field intensity and direction are due to diamagnetic currents that are carried by ions which drift in a sheath as the result of gradients in the magnetic field and in the plasma pressure within the sheath. The thickness of the sheaths that we consider is approximately a few ion Larmor radii. An electric field is normal to the magnetic field in the sheath. Solutions of Vlasov's equation and Maxwell's equations are presented which account for several types of magnetic holes, including 'null sheets,' that have been observed.

1. Introduction

In an analysis of high-resolution (12.5 samples/s) magnetic field measurements obtained by Explorer 43 in the period March 18 to April 9, 1971, *Turner et al.* [1977] found that most low-field intensity regions ($B \leq 1 \gamma$) were isolated and very thin ($\approx 10^4$ km, or $\approx 100 R_L$, where R_L is the proton Larmor radius). They called these regions magnetic holes. Observations of such structures with two spacecraft [*Fitzenreiter and Burlaga*, 1978] show that the extent of magnetic holes is more than $\approx 10^5$ km. Magnetic holes form a class of current sheets.

Three types of magnetic holes were identified by *Turner et al.* [1977] and analyzed by *Fitzenreiter and Burlaga* [1978]: (1) holes with no change in the magnetic field direction across the current sheet, (2) holes with a reversal in magnetic field direction but no rotation of the field vector across the current sheet, and (3) holes in which there is a rotation of the magnetic field vector across the current sheet. Turner et al. also exhibited current sheets in which the magnetic field intensity increased with no change in direction ('antiholes'). The purpose of this paper is to apply the theory presented previously by *Lemaire and Burlaga* [1976] to explain antiholes and the three types of magnetic holes.

For the calculations we make the following assumptions:

1. Magnetic holes are stationary inhomogeneities convected with the solar wind speed.

2. They are bounded by thin current sheaths, and the radius of curvature of these sheaths is very large in comparison with the thickness. As a consequence, we consider the geometry of the sheath to be planar, with a normal in the $\hat{z}$ direction.

3. The physical variables are functions only of z.

4. The magnetic field $\mathbf{B}(z)$ is normal to the $\hat{z}$ direction as for tangential discontinuities.

5. In the frame of reference moving with the magnetic hole there is an electric field $\mathbf{E}(z)$ along $\hat{z}$; i.e., $E_x = E_y = 0$. This implies that there is no net plasma flow across the boundary layer.

6. The plasma is quasi-neutral and consists of electrons and protons. Multiionic plasmas have been considered but will not be discussed in this paper.

7. The plasma is collisionless.

8. The diamagnetic currents are carried only by the protons (the electron velocity distribution is assumed to be isotropic).

9. The plasma is in thermal equilibrium on both sides of the current sheath, and the bulk velocities at $z = \pm\infty$ are both equal to zero in a frame of reference comoving with the solar wind speed.

The basic equations are Maxwell's and Vlasov's equations. We obtained solutions of these equations, which describe magnetic holes, using the method described by *Lemaire and Burlaga* [1976]. In all of the examples discussed below we assume that the ambient magnetic intensity and particle density on each side of the current sheet are 5 γ (nT) and 5 protons or electrons per cubic centimeter, respectively. For simplicity we also assume that the temperatures of the electrons and ions are the same on both sides of the layer at $z = \pm\infty$: $T_e = T_i = 7.5 \times 10^4$ K. Calculations with $T_e \neq T_i$ and with different temperatures on both sides have also been made but are not discussed in this paper. This complicates the structure of the layer but does not alter the basic physical effects, which are our principal interest for the present article. The following sections present solutions to the problems that we have posed above, and they include heuristic discussions, based on particle orbit theory, aimed at identifying the basic physical processes in magnetic holes.

2. Magnetic Holes With No Change in $\hat{B}$: $\Delta\omega = 0$

Let us consider magnetic holes in which the direction of magnetic field remains along $\hat{x}$: $\mathbf{B} = B(z)\hat{x}$. In particular, consider the case where $B = 1 \gamma$ (nT) in the middle of the hole, together with the other boundary conditions discussed in section 1. A self-consistent solution of Vlasov's equation and Maxwell's equations, obtained by the method of *Lemaire and Burlaga* [1976], is shown in Figure 1.

The current in Figure 1 reaches a maximum at the two points where $|dB/dz|$ is largest. This follows directly from

$$\mu_0 \mathbf{J} = \nabla \times \mathbf{B} = \hat{y}\frac{dB_x}{dz} = \hat{y}\frac{dB}{dz}$$

Note that $\mathbf{J}$ flows normal to $\mathbf{B}$ and $\hat{z}$ in this current sheet. In the middle of the magnetic hole, $|\mathbf{J}|$ is zero because dB_x/dz goes to
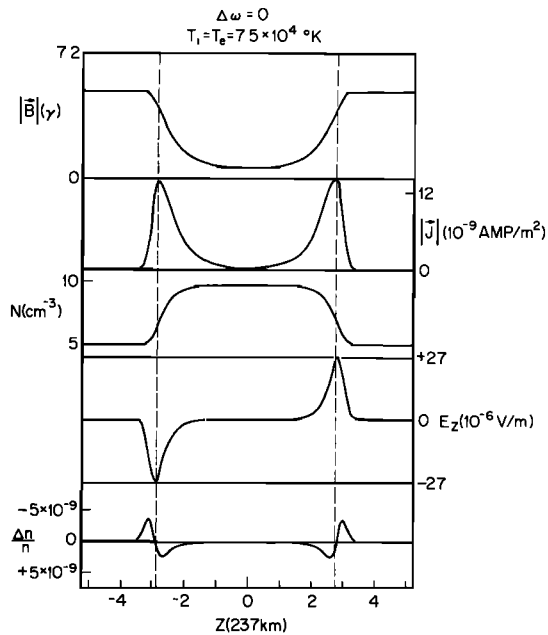
Fig. 1.   Model of an isothermal magnetic hole in which $|\mathbf{B}|$ decreases to $1\ \gamma$ without changing direction and then increases symmetrically to its initial value.

zero there as J_y changes from negative values to positive values.

In the first-orbit approximation, $\mathbf{J}$ is actually the sum of two currents, the gradient drift current

$$J_D = -\frac{W_\perp}{B^2}\frac{dB}{dz}$$

(where $W_\perp = \Sigma\ \tfrac{1}{2}mv_\perp^2 = Nk(T_{i\perp} + T_{e\perp})$, which results from the gradient drift of protons in the inhomogeneous field, and the magnetization current

$$J_M = \frac{-d}{dz}\left(\frac{W_\perp}{B}\right)$$

(There is no current due to $\mathbf{E}$, since electrons and protons drift in the same direction and with the same speed due to $\mathbf{E} \times \mathbf{B}$.) Setting $\mu_0(J_D + J_M) = \nabla \times \mathbf{B}$ gives

$$\frac{B^2}{2\mu_0} + Nk(T_{i\perp} + T_{e\perp}) = \text{const} \qquad (1)$$

which shows that the pressure is constant across the current sheet, in agreement with our assumption of equilibrium. The increase in N coincident with the decrease in B shown in Figure 1 is a consequence of the constant pressure condition (1), since for the case considered the kinetic temperature is nearly constant across the sheath.

In the example illustrated in Figure 1 we assumed that the kinetic pressure enhancement was due to a larger thermal proton and electron density inside the magnetic hole. But a similar structure would be obtained when the excess of particle pressure is due to a localized beam of suprathermal electrons or ions spiraling in an interplanetary magnetic flux tube. High-intensity electron spikes or proton burst events sporadically detected in the interplanetary medium can produce such an excess kinetic pressure in an otherwise uniform solar wind plasma. Correlative studies would however be necessary to verify if some of the observed magnetic holes can be associated with these suprathermal particle beams.

The electric field E_z in Figure 1 preserves local quasi-neutrality in the plasma. Its value is largest where $|dN/dz|$ is largest. This can be understood heuristically as follows. The electron velocity distribution is assumed to be isotropic. This implies that the bulk velocity of the electrons is zero and that their pressure tensor is isotropic with $p_e = NkT_e$. The momentum equation for the electrons is therefore given by

$$\frac{dp_e}{dz} = -N|e|E_z = kT_e\frac{dN}{dz} + N\frac{dkT_e}{dz}$$

which shows that the charge separation electric field is indeed proportional to $|d \ln N/dz|$ when $dT_e/dz \simeq 0$; this is the case for the solution in Figure 1. If the temperature changed and N were everywhere constant, the same argument would apply, and the $|\mathbf{E}|$ needed to maintain equilibrium in this case would be greatest where $|dT/dz|$ was greatest. In general, both $N(z)$ and $T(z)$ can vary, and they need not be in phase; in this case, $E_z(z)$ could be complicated, but the physical processes would be basically the same as those in the simpler cases just described.

The first inflection point in $N(z)$ in Figure 1 is indicated by a dashed line; note the small accumulation of positive charge at a distance of approximately R_{L2} (the proton Larmor radius on side 2) to the right of this point and the small accumulation of negative charge at $\approx R_{L1}$ to the left of this point. Since $B_1 > B_2$, $R_{L1} < R_{L2}$, and the peak of negative excess charge is closer to the inflection point of N than the peak of positive excess charge. This accounts for the asymmetry in the $E_z(z)$ profile in Figure 1.

A charge separation $\Delta n/N$ is required to support $\mathbf{E}$. Poisson's equation gives $|e|\Delta n = dE_z/dz$ or $\Delta n \propto -d^2N/dz^2$, indicating that there will be an accumulation of negative charge in the region where E_z is decreasing most rapidly (i.e., where the dN/dz is increasing with z) and an accumulation of positive charge where E_z is increasing most rapidly (i.e., where dN/dz is decreasing with z). Such electrostatic double layers generally appear at the surface of a magnetic hole having an excess kinetic plasma pressure. The excess of positive charges at the edges of a dense plasma region results from the larger gyroradius of the ions compared with the gyroradius of the electrons. Indeed, the positive charges are deflected at a larger distance from the interior of the density (or pressure) enhancement than the lighter negative charges. On the contrary, an excess of negative charges is expected to accumulate at the edge of a plasma depression. Indeed, because of their small mass-to-charge ratio the electrons tend to be reflected before the ions. This builds up a negative surface charge on the low-density side and a positive charge accumulation toward the high-density side (see Figure 2a).

Willis [1971, 1975] has discussed the charge separation electric field in a Ferraro-type magnetopause boundary layer,
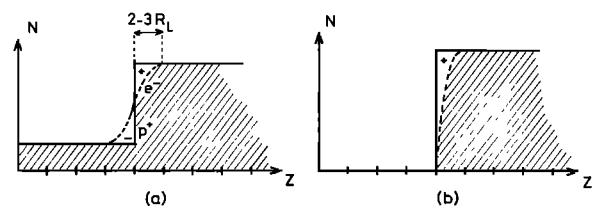

Fig. 2.   An illustration of the charge accumulation which produces an electric field in a magnetic hole and which determines the thickness of a magnetic hole. (a) A low density on one side and a high density on the other side of a sheath. (b) Zero density on one side of the sheath.
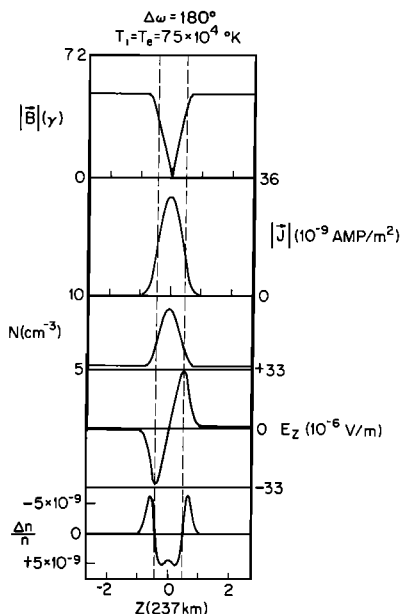
Fig. 3. Mode of an isothermal magnetic hole in which the direction of **B** reverses without a rotation of $\hat{B}$.

assuming that there is no plasma in the magnetosphere (i.e., on the low-density side). In this extreme case when the density is strictly equal to zero outside the plasma region, only the positive charge accumulation is present at the edge of the enhancement (see Figure 2b). This 'single-layer' structure is also described by the kinetic theory of *Lemaire and Burlaga* [1976] when the plasma density is forced to become equal to zero at $z = +\infty$.

3. HOLES WITH A REVERSAL IN FIELD DIRECTION WITHOUT ROTATION: $\Delta\omega = 180°$

Let us again consider the case where $\mathbf{B} = B(z)\hat{x}$, but now we allow $B(z)$ to vary monotonically from $B_1 > 0$ to $B_2 < 0$. Clearly, $B(z)$ must go through zero at some point in the magnetic hole in this case. Note that 'neutral sheets' or 'null sheets' ideally correspond to this special case of magnetic field reversal without rotation. As before, let us take $B_1 = 5\,\gamma$, $B_2 = -5\,\gamma$, $N_e = N_p = 5/\text{cm}^3$, and $T_i = T_e = \text{const} = 7.5 \times 10^4$ K on each side of the current sheet.

Figure 3 shows one possible solution of Vlasov's equation and Maxwell's equations for the case considered. One sees that there is a single current peak, which is maximum in the center of the diamagnetic current layer, where $|\mathbf{B}| = 0$. The density rises to a maximum at the center of the hole, as required by the pressure balance condition for equilibrium. The charge separation electric field is maximum in each of the two regions where N changes most rapidly, as required to maintain approximate local quasi-neutrality of the plasma. Each electric field region is maintained by a concentration of positive charge on one side of the maximum of $|\mathbf{E}|$ and a concentration of negative charge on the other side; note that the positive charge concentrations overlap. Although the appearance of the magnetic hole in this case is rather different from that in section 2, the basic physical processes are the same in both cases.

Figure 4 shows another solution of the Vlasov-Maxwell equations, again for $\mathbf{B} = B(z)\hat{x}$ and for the same boundary conditions that were used in the preceding example. Although Figures 3 and 4 are solutions for the same boundary value problem, the solution in Figure 4 is rather different from that
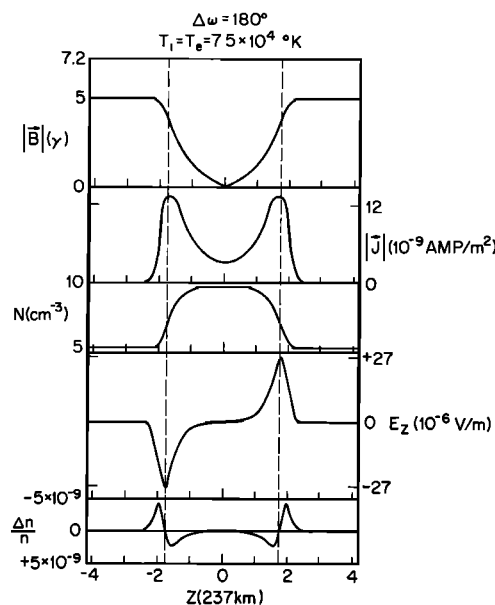

Fig. 4. Another isothermal magnetic hole in which the direction of **B** reverses without a rotation of $\hat{B}$. Although the boundary conditions are the same as those for the hole in Figure 3, the structures of the two holes are very different, illustrating the nonuniqueness of solutions of Vlasov's equation.

in Figure 3. This illustrates the well-known point that boundary conditions do not specify a unique solution to the Vlasov-Maxwell equations. The principal difference in this case is that Figure 4 shows a double layer current distribution, while Figure 3 shows a single peaked current distribution. The current distribution in Figure 4 resembles that in Figure 1 in being double peaked, and it resembles that in Figure 3 in having a nonzero current where B is a minimum.

4. MAGNETIC HOLES WITH A ROTATION OF B

Consider the case in which **B** rotates 180° from one side of a magnetic hole to the other, and consider the same boundary conditions that were used in our previous examples. A solution of the Vlasov-Maxwell equations obtained by our numerical program is shown in Figure 5. The magnetic field intensity
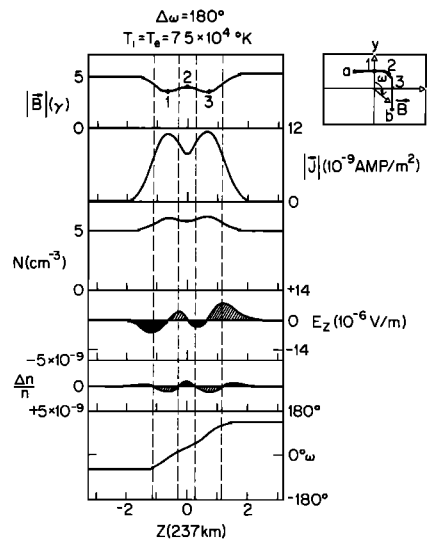

Fig. 5. Model of an isothermal magnetic hole in which the direction of **B** changes by a rotation of $\hat{B}$ through 180°. In this case there is a component of current along **B** due to the rotation as well as a component of current normal to **B** due to the gradients.
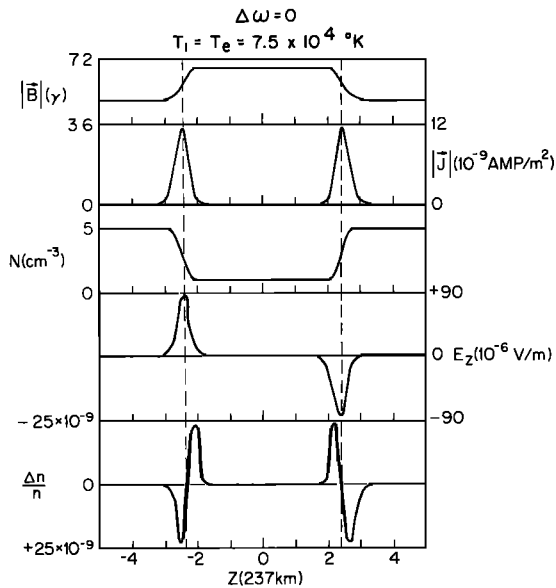
Fig. 6.   Model of an isothermal antihole. Compare with the hole in Figure 1.

profile in this case differs qualitatively from those considered above in that there is now a secondary maximum in B where in previous examples B was a minimum. The reason for the secondary maximum is basically geometrical, as can be seen by considering the rotation of $\mathbf{B}$ in the current sheet (see the insert in Figure 5). When $\mathbf{B}$ rotates in a plane, the current has a component parallel to the local magnetic field direction as well as a component perpendicular to $\mathbf{B}$:

$$\mu_0 \mathbf{J} = \hat{y} \frac{dB_x}{dz} - \hat{x} \frac{dB_y}{dz} = (\hat{z} \times \hat{B}) \frac{dB}{dz} + \mathbf{B} \frac{d\omega}{dz}$$

where $B_x = B \sin \omega$ and $B_y = B \cos \omega$. Therefore if the magnetic field rotates without changing intensity (i.e., $dB/dz = 0$), the diamagnetic current $\mathbf{J}$ is field aligned and proportional to the rate of rotation $d\omega/dz$. In Figure 5 the peaks in $\mathbf{J}$ occur near the points where the direction ω changes most rapidly (and where dB/dz happens to be zero, as can be seen in the insert in Figure 5). $\mathbf{J}$ is also nonzero at the secondary maximum of B even though $dB/dz = 0$ there because the direction of $\mathbf{B}$ is changing ($d\omega/dz \neq 0$) at that point.

The density profile in Figure 5 is anticorrelated with $B(z)$ as required by the constant pressure condition. The electric field is again extremal at the extrema of dN/dz for the same reasons given earlier. The charge separation profile shows a positive and negative peak beside each extremum of E_z, as required to maintain E_z, and the charge peaks are separated from the peaks in E_z by $\approx 1\ R_L$.

5.   ANTIHOLES

Figure 6 shows a solution of the Vlasov-Maxwell equations for a linear 'antihole' for the same boundary conditions that we have used in previous examples. By definition, B is enhanced in some region with dimensions of the order of several ion Larmor radii or more. Since $\mathbf{B} = B\hat{z}$, $|\mathbf{J}|$ is maximum

where dB/dz is extremum. We have assumed $T = $ const, so N is anticorrelated with B as required by the pressure balance condition. E_z is again extremum where dN/dz is extremum, and each peak in E is maintained by a charge separation over a distance of a few Larmor radii. Thus this type of antihole is physically equivalent to the type of magnetic hole described in Figure 1.

6.   CONCLUSIONS

Magnetic holes are considered here as kinetic scale plasma inhomogeneities convected with the solar wind speed. These localized density and/or temperature enhancements are assumed to be sheetlike structures which are stationary in the solar wind flow. The plasma in the magnetic hole is separated from the background solar wind by sheaths whose thicknesses are only a few proton gyroradii. Diamagnetic currents flow in these sheaths. In the kinetic model presented here to describe the structure of these sheaths, we have assumed that the radius of curvature of the surface is much larger than the thickness of the current sheath itself. Neglecting Coulomb collisions and other irreversible processes, we have found, by using the models of Lemaire and Burlaga [1976], a variety of magnetic field structures similar to those observed in solar wind magnetic holes and antiholes. Even null sheets, in which the magnetic field reverses with $|\mathbf{B}|$ going strictly through zero, can be modeled by the theory presented above (e.g., case 3).

There are a number of other factors that might be considered in constructing more refined models of magnetic holes. Coulomb collisions, although infrequent, would tend to broaden the holes. In some cases the ion drift speed might exceed the Alfvén speed and cause local instabilities. Variations in both ion density and temperature should be considered. The effects of alpha particle drifts and curvature of the current sheet might also be significant in some cases. These factors are essentially complications, however. The aim of this paper has been to explain the basic mechanisms responsible for magnetic holes. It will be appropriate to consider the other factors when high-resolution plasma observations are available which give $n(z)$, $T(z)$, etc., in the magnetic holes.

REFERENCES

Fitzenreiter, R., and L. F. Burlaga, Structure of current sheets in magnetic holes at 1 AU, J. Geophys. Res., 83, in press, 1978.
Lemaire, J., and L. F. Burlaga, Diamagnetic boundary layers: A kinetic model, Astrophys. Space Sci., 45, 303-325, 1976.
Turner, J. M., L. F. Burlaga, N. F. Ness, and J. Lemaire, Magnetic holes in the solar wind, J. Geophys. Res., 82, 1921-1924, 1977.
Willis, D. M., Structure of the magnetopause, Rev. Geophys. Space Phys., 9, 953-985, 1971.
Willis, D. M., Microstructure of the magnetopause, Geophys. J. Roy. Astron. Soc., 41, 355-389, 1975.